



Cite this: *Polym. Chem.*, 2016, 7, 1545

Received 5th January 2016,
Accepted 26th January 2016

DOI: 10.1039/c6py00023a

www.rsc.org/polymers

Dithieno[2,3-*d*;2',3'-*d*]benzo[2,1-*b*;3,4-*b'*]-dithiophene: a novel building-block for a planar copolymer†

Ashok Keerthi,^a Cunbin An,^a Mengmeng Li,^a Tomasz Marszalek,^a Antonio Gaetano Ricciardulli,^a Boya Radha,^b Fares D. Alsewaleim,^c Klaus Müllen^a and Martin Baumgarten^{*a}

A planar heteroacene building block, dithieno[2,3-*d*;2',3'-*d*]benzo[1,2-*b*;3,4-*b'*]dithiophene (DTmBDT), is reported via a facile synthetic procedure. Single-crystal X-ray diffraction of Br₂-DTmBDT reveals that dodecyl chains interdigitate, still enabling close π -stacking of 3.42 Å. A very high molecular weight quasi-planar copolymer PDTmBDT-DPP exhibited a high hole mobility of 0.36 cm² V⁻¹ s⁻¹ in preliminary studies of organic field-effect transistors.

Conjugated molecules have become popular in the recent years for their applications mainly in organic electronics¹ [organic light emitting diodes (OLEDs), organic field-effect transistors (OFETs), and organic photovoltaics (OPVs)] due to their tunable structure, solution processability and thermal stability along with their advantages of flexibility, lightweight, and low-cost for use in large-area displays, sensors, detectors, and light harvesting devices.² In the recent years, there has been tremendous progress in the development of heteroacenes, fused conjugated molecules and their corresponding polymers towards attaining high charge carrier mobilities.^{3–6} However, the device performance needs to be improved with a modified synthetic design of polymers for simple processing technologies, which remains an essential task.^{7,8}

Earlier investigations have shown that the planarization and energy levels of copolymers can be tuned by the choice of respective donor (D) and acceptor (A) comonomers.^{9–11} Recent developments in D–A copolymers consisting of fused planar molecules as donors and electron-acceptors such as naphthalene diimide (NDI),^{12,13} diketopyrrolopyrrole (DPP),^{14–17} and 2,1,3-benzothiadiazole (BTZ),^{9,18,19} have shown significant pro-

gress in OFETs and OPVs. Moreover, among the class of π -extended ring-fused heteroacenes, thiophene-based heteroacene⁶ donors especially those with thieno[3,2-*b*]thiophene (TT) units have gained much importance.^{19–24}

In the quest for developing heteroatom containing acenes, we have reported five-ring-fused pentacene analogs, benzo[1,2-*b*;4,5-*b'*]bis[*b*]benzothiophene (BBBT),²⁵ dithieno[2,3-*d*;2',3'-*d'*]benzo[1,2-*b*;4,5-*b'*]dithiophene (DTBDT)²⁶ and heptacene analog dithienothieno[2,3-*d*;2',3'-*d'*]benzo[1,2-*b*;4,5-*b'*]dithiophene (DTTBDT)²⁷ (Fig. 1). However, introducing solubilizing groups on the central core of these molecules will disturb the π -stacking. In this work, we present the facile synthesis of a novel didodecyl substituted tetrathiapentacene donor unit, dithieno[2,3-*d*;2',3'-*d'*]benzo[1,2-*b*;3,4-*b'*]dithiophene (DTmBDT). The current versatile building block DTmBDT can be easily made soluble with dodecyl side chains at the central benzene ring and functionalized with halogens in the alpha positions of the outer thiophenes for further reactions. We demonstrate the potential of this highly soluble heteropentacene donor unit by copolymerization with 2,5-bis(2-octyldodecyl)-3,6-di(thiophen-2-yl)-2,5-dihydropyrrolo[3,4-*c*]pyrrole-1,4-dione (DPP) as an electron-acceptor.

The synthetic route of PDTmBDT-DPP is sketched in Scheme 1. First thieno[3,2-*b*]thiophene (1) was converted to

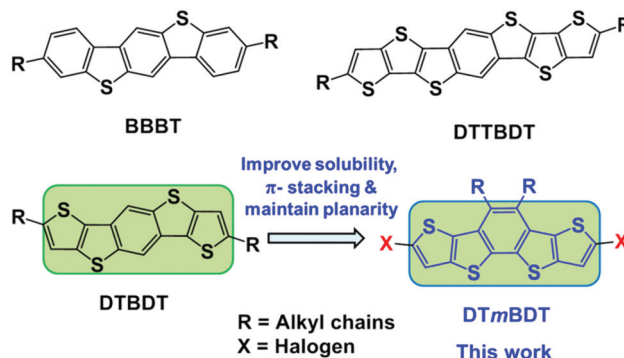


Fig. 1 Thiophene fused heteroacene molecules.

^aMax Planck Institute for Polymer Research, Ackermannweg 10, 55128 Mainz, Germany. E-mail: martin.baumgarten@mpip-mainz.mpg.de

^bSchool of Physics and Astronomy, Condensed Matter Physics Group, the University of Manchester, M13 9PL Manchester, UK

^cPetrochemical Research Institute, King Abdulaziz City of Science and Technology, PO Box 6086, Riyadh 11442, Saudi Arabia

† Electronic supplementary information (ESI) available: Detailed experimental and computational data. CCDC 1435119. For ESI and crystallographic data in CIF or other electronic format see DOI: 10.1039/c6py00023a





Scheme 1 Synthesis of the new donor molecular building block and PDTmBDT-DPP copolymer.

2,5-dibromothiopheno[3,2-*b*]thiophene (2) *via* bromination and selective monosilylation which was carried out using *n*-BuLi followed by the reaction with trimethylsilylchloride to yield (5-bromothiopheno[3,2-*b*]thiophen-2-yl)trimethylsilane (3). Then the lithium diisopropylamide (LDA) induced migration of bromides of compound 3 to the β -position and dimerization using CuCl_2 were accomplished in a one-pot reaction to acquire dimer 4. The planarized and ring closed derivative 6 was achieved through the Suzuki–Miyaura coupling reaction of dimer 4 and 1,2-didodecyl ethenyl diboronate 5 in 84% yield. The disilane derivative was then converted to the dibromo derivative $\text{Br}_2\text{-DTmBDT}$ in 95% yield using *N*-bromosuccinimide (NBS).

According to our previous work,²⁸ tri-*tert* butylphosphoniumtetrafluoroborate ($(t\text{-Bu})_3\text{P}\cdot\text{HBF}_4$) is an effective ligand to yield high molecular weights with $\text{Pd}_2(\text{dba})_3$ in Suzuki couplings based on diketopyrrolopyrrol diboronate (7). Therefore, the same polymerization conditions were used to synthesize the copolymer PDTmBDT-DPP *via* the Suzuki polymerization reaction between the building block $\text{Br}_2\text{-DTmBDT}$ and DPP diboronate 7. After purification on a Soxhlet extractor with methanol, acetone and hexane to remove the oligomeric fractions and final extraction with chloroform, the highest molecular weight polymer was achieved ($M_n = 308.9$ kDa and $M_w = 976.4$ kDa against polystyrene standards in THF). However, polydispersity (PDI = 3.2)

of the polymer was found to be slightly high which might be due to aggregation of highly planar polymeric segments.

Single crystal XRD analysis of $\text{Br}_2\text{-DTmBDT}$ revealed that these crystals were packed in the $P2_1/c$ (monoclinic) space group (Fig. 2). It was found that the $\text{Br}_2\text{-DTmBDT}$ is a completely planar structure and forms a dyad between two molecular planes in a face-to-face manner with a π - π distance of 3.42 Å and follows a “herringbone” pattern of dyads. Interestingly, these two



Fig. 2 Crystal structure and packing patterns of $\text{Br}_2\text{-DTmBDT}$: (a) crystal structure, (b) alkyl chain interdigitation and close packing, (c) π - π interactions in the dyad and (d) the top view of the dyad.



molecules in one dyad only overlap through the TT units (Fig. 2d). Most surprisingly, the dodecyl chains of the neighboring molecules were packed in an interdigitating manner.

The solution state absorption spectrum of **PDTmBDT-DPP** in TCB shows a maximum absorption wavelength (λ_{\max}) at 753 nm with a shoulder peaking at 685 nm (Fig. 3a). The λ_{\max} is attributed to intramolecular charge transfer (ICT) between the donor and acceptor in the polymer backbone (Fig. S2a†).²⁹ The thin film of **PDTmBDT-DPP** prepared by drop-casting a TCB solution onto a quartz plate displayed the same absorption wavelength but with higher intensities of the shoulder peaks at a lower absorption wavelength compared to that in solution. The optical bandgap of **PDTmBDT-DPP** derived from the onset of the absorption spectrum of the film is 1.51 eV. The predicted (TD-SCF) UV-vis absorption spectra suggest that the effective conjugation might be extended up to three repeating units of the copolymer (ESI, Fig. S2b†).

The electrochemical properties of the polymer were investigated by cyclic voltammetry of drop-cast films on an ITO substrate. **PDTmBDT-DPP** showed multiple oxidations (Fig. 3b).



Fig. 3 (a) UV-vis absorption spectra at room temperature (dotted line – drop cast thin film absorption on the quartz plate, thick line – dilute solution absorption in TCB), (b) cyclic voltammetric profile (in 0.1 M Bu_4NPF_6 in dichloromethane as the supporting electrolyte with a scan rate of 100 mV s^{-1} and the potentials reported are versus the Fc^+/Fc redox couple as an external standard) of **DTmBDT** copolymer.

The first oxidation ($E_{\text{ox1}}^{1/2}$) occurred at 0.66 V with an onset potential of 0.27 V leading to an ionization potential (IP) of -5.07 eV . The first reduction ($E_{\text{red1}}^{1/2}$) of the polymer appeared at -1.54 V by showing an onset potential at 1.27 V and the electron affinity (EA) was found to be -3.53 eV . The IP and EA energy levels are calculated from the respective first oxidation and reduction onset potentials and the electrochemical energy gap (1.54 eV) is quite close to the optical bandgap. It was found from the density functional theory (DFT) calculations (B3LYP, 6-31G(d)) of the frontier orbitals that the HOMO is distributed over the two **DPP** units and one **DTmBDT** unit. However, the **DPP** units (Fig. S3–S5†) majorly contribute to the LUMO. Interestingly, the dihedral angles between the **DPP** and **DTmBDT** units were found to be 2–3 degrees leading to a quasi-planar polymer backbone (ESI†).

TGA analysis revealed that the polymer was stable up to $410 \text{ }^\circ\text{C}$ with only 2% weight loss under a nitrogen atmosphere (Fig. S9a†). DSC analysis showed that **PDTmBDT-DPP** has a high glass transition temperature (T_g) of $189 \text{ }^\circ\text{C}$ and a segmental melting point at $331 \text{ }^\circ\text{C}$ along with a corresponding crystallization peak at $311 \text{ }^\circ\text{C}$ while cooling (Fig. S9b†).

The charge carrier transport of **PDTmBDT-DPP** was investigated using bottom-gate bottom-contact configuration OFET devices with 50 nm-thick Au electrodes as the source and drain and 300 nm-thick SiO_2 as the dielectric source. The semiconducting **PDTmBDT-DPP** layer was drop-cast from a chloroform solution at a concentration of 2 mg ml^{-1} . In order to remove the residual solvent in the drop-cast thin film, annealing was performed at $100 \text{ }^\circ\text{C}$ for 30 min. All electrical measurements were performed under a nitrogen atmosphere. The transfer (Fig. 4) and output (Fig. S10†) characteristics indicated a typical linear saturation behavior. From the transfer plots, hole transport is observed with the mobility of $0.36 \text{ cm}^2 \text{ V}^{-1} \text{ s}^{-1}$ and the on/off ratio reaches 10^5 .

The polymer organization of the **PDTmBDT-DPP** drop-cast film on the silicon dioxide dielectric surface of the transistor was investigated by grazing incidence wide-angle X-ray scattering (GIWAXS). The **PDTmBDT-DPP** film showed a high degree



Fig. 4 OFET transfer characteristics.



of order in the out-of-plane direction (along q_z for $q_{xy} = 0 \text{ \AA}^{-1}$) as indicated by reflections up to the third order (Fig. S11†). These scattering intensities confirmed a typical lamellar organization with a high long-range order on the surface with an interlayer distance of $\sim 2.18 \text{ nm}$. A similar trend of layered behavior was observed in the AFM analysis of the OFET device (Fig. S12†). The wide-angle in-plane reflection was assigned to a π -stacking distance of 3.7 \AA of the edge-on arranged conjugated backbones.³⁰ In this edge-on organization, the π -stacking direction is oriented parallel to the surface, which is beneficial for charge carrier transport in field-effect transistors.

In summary, we have synthesized a novel fused tetrathia-pentacene building block with solubilizing side chains not hindering the π -stacking and a corresponding copolymer **PDTmBDT-DPP**. This polymer exhibited a very high molecular weight, highly planar back-bone and excellent thermal stability up to $430 \text{ }^\circ\text{C}$. For the new heteroacene with dodecyl side chains, very good π -stacking (3.4 \AA) and alkyl side chain interdigitation were found from the single crystal analysis making this donor molecule itself promising for future independent OFET studies and also for the synthesis of planar copolymers with different acceptors. In first device experiments with **PDTmBDT-DPP**, we have demonstrated the high charge carrier mobilities of $0.36 \text{ cm}^2 \text{ V}^{-1} \text{ s}^{-1}$. These preliminary results are highly promising towards solution processable OFET applications, and complete investigations on device optimization and performance including OPV characterization are in progress in our laboratory.

The authors want to thank Wojciech Pisula for first OFET studies performed by M. L. Thanks to Dr Dieter Schollmeyer at Johannes Gutenberg-University, Mainz for crystal structure analysis and Jutta Schnee for helping in the synthesis of thieno[3,2-*b*]thiophene derivatives. B. R. would like to acknowledge the FP7 MC-fellowship. KACST is highly acknowledged for financial support.

Notes and references

- X. Guo, M. Baumgarten and K. Müllen, *Prog. Polym. Sci.*, 2013, **38**, 1832–1908.
- Y. Zhao, Y. Guo and Y. Liu, *Adv. Mater.*, 2013, **25**, 5372–5391.
- I. Kang, H.-J. Yun, D. S. Chung, S.-K. Kwon and Y.-H. Kim, *J. Am. Chem. Soc.*, 2013, **135**, 14896–14899.
- G. Kim, S.-J. Kang, G. K. Dutta, Y.-K. Han, T. J. Shin, Y.-Y. Noh and C. Yang, *J. Am. Chem. Soc.*, 2014, **136**, 9477–9483.
- B. Sun, W. Hong, Z. Yan, H. Aziz and Y. Li, *Adv. Mater.*, 2014, **26**, 2636–2642.
- K. Takimiya, S. Shinamura, I. Osaka and E. Miyazaki, *Adv. Mater.*, 2011, **23**, 4347–4370.
- H.-R. Tseng, H. Phan, C. Luo, M. Wang, L. A. Perez, S. N. Patel, L. Ying, E. J. Kramer, T.-Q. Nguyen, G. C. Bazan and A. J. Heeger, *Adv. Mater.*, 2014, **26**, 2993–2998.
- H. Sirringhaus, *Adv. Mater.*, 2014, **26**, 1319–1335.
- M. Zhang, H. N. Tsao, W. Pisula, C. Yang, A. K. Mishra and K. Müllen, *J. Am. Chem. Soc.*, 2007, **129**, 3472–3473.
- J.-S. Wu, S.-W. Cheng, Y.-J. Cheng and C.-S. Hsu, *Chem. Soc. Rev.*, 2015, **44**, 1113–1154.
- M. E. Cinar and T. Ozturk, *Chem. Rev.*, 2015, **115**, 3036–3140.
- X. Guo, A. Facchetti and T. J. Marks, *Chem. Rev.*, 2014, **114**, 8943–9021.
- M. Yuan, M. M. Durban, P. D. Kazarinoff, D. F. Zeigler, A. H. Rice, Y. Segawa and C. K. Luscombe, *J. Polym. Sci., Part A: Polym. Chem.*, 2013, **51**, 4061–4069.
- P. Sonar, S. P. Singh, Y. Li, M. S. Soh and A. Dodabalapur, *Adv. Mater.*, 2010, **22**, 5409–5413.
- C. B. Nielsen, M. Turbiez and I. McCulloch, *Adv. Mater.*, 2013, **25**, 1859–1880.
- X. Guo, S. R. Puniredd, M. Baumgarten, W. Pisula and K. Müllen, *Adv. Mater.*, 2013, **25**, 5467–5472.
- H. Bürckstümmer, A. Weissenstein, D. Bialas and F. Würthner, *J. Org. Chem.*, 2011, **76**, 2426–2432.
- C. Luo, A. K. K. Kyaw, L. A. Perez, S. Patel, M. Wang, B. Grimm, G. C. Bazan, E. J. Kramer and A. J. Heeger, *Nano Lett.*, 2014, **14**, 2764–2771.
- L. Biniek, B. C. Schroeder, J. E. Donaghey, N. Yaacobi-Gross, R. S. Ashraf, Y. W. Soon, C. B. Nielsen, J. R. Durrant, T. D. Anthopoulos and I. McCulloch, *Macromolecules*, 2013, **46**, 727–735.
- C. Wetzel, E. Brier, A. Vogt, A. Mishra, E. Mena-Osteritz and P. Bäuerle, *Angew. Chem., Int. Ed.*, 2015, **54**, 12334–12338.
- Y. Tsutsui, T. Sakurai, S. Minami, K. Hirano, T. Satoh, W. Matsuda, K. Kato, M. Takata, M. Miura and S. Seki, *Phys. Chem. Chem. Phys.*, 2015, **17**, 9624–9628.
- J. Shaw, H. Zhong, C. P. Yau, A. Casey, E. Buchaca-Domingo, N. Stingelin, D. Sparrowe, W. Mitchell and M. Heeney, *Macromolecules*, 2014, **47**, 8602–8610.
- J. Zhang, K. Zhang, W. Zhang, Z. Mao, M. S. Wong and G. Yu, *J. Mater. Chem. B*, 2015, **3**, 10892–10897.
- L. Huo, T. Liu, X. Sun, Y. Cai, A. J. Heeger and Y. Sun, *Adv. Mater.*, 2015, **27**, 2938–2944.
- P. Gao, D. Beckmann, H. N. Tsao, X. Feng, V. Enkelmann, W. Pisula and K. Müllen, *Chem. Commun.*, 2008, 1548–1550.
- P. Gao, D. Beckmann, H. N. Tsao, X. Feng, V. Enkelmann, M. Baumgarten, W. Pisula and K. Müllen, *Adv. Mater.*, 2009, **21**, 213–216.
- L. Chen, M. Baumgarten, X. Guo, M. Li, T. Marszalek, F. D. Alsewaleim, W. Pisula and K. Müllen, *J. Mater. Chem. B*, 2014, **2**, 3625–3630.
- C. An, T. Marszalek, X. Guo, S. R. Puniredd, M. Wagner, W. Pisula and M. Baumgarten, *Polym. Chem.*, 2015, **6**, 6238–6245.
- J.-S. Wu, C.-T. Lin, C.-L. Wang, Y.-J. Cheng and C.-S. Hsu, *Chem. Mater.*, 2012, **24**, 2391–2399.
- I. Osaka and K. Takimiya, *Polymer*, 2015, **59**, A1–A15.

